Published in final edited form as:
J Inherit Metab Dis. 2012 September ; 35(5): 847–857. doi:10.1007/s10545-011-9446-x.

Combination small molecule PPT1 mimetic and CNS-directed gene therapy as a treatment for infantile neuronal ceroid lipofuscinosis

Marie S. Roberts[1], **Shannon L. Macauley**[1], **Andrew M. Wong**[2], **Denis Yilmas**[2], **Sarah Hohm**[1], **Jonathan D. Cooper**[2], and **Mark S. Sands**[1]

[1] Department of Internal Medicine, Washington University School of Medicine, Campus Box 8007, 660 S. Euclid Ave., St. Louis, MO 63110, USA.

[2] Pediatric Storage Disorders Laboratory, Department of Neuroscience and MRC Center for Neurodegeneration Research, Institute of Psychiatry, King's College London, London SE5 9NU, UK

Abstract

Infantile neuronal ceroid lipofuscinosis (INCL) is a profoundly neurodegenerative disease of children caused by a deficiency in the lysosomal enzyme palmitoyl protein thioesterase-1 (PPT1). There is currently no effective therapy for this invariably fatal disease. To date, preclinical experiments using single treatments have resulted in incremental clinical improvements. Therefore, we determined the efficacy of CNS-directed AAV2/5-mediated gene therapy alone and in combination with the systemic delivery of the lysosomotropic PPT1 mimetic phosphocysteamine. Since CNS-directed gene therapy provides relatively high levels of PPT1 activity to specific regions of the brain, we hypothesized that phosphocysteamine would complement that activity in regions expressing sub therapeutic levels of the enzyme. Results indicate that CNS-directed gene therapy alone provided the greatest improvements in biochemical and histological measures as well as motor function and life span. Phosphocysteamine alone resulted in only minor improvements in motor function and no increase in lifespan. Interestingly, phosphocysteamine did not increase the biochemical and histological response when combined with AAV2/5-mediated gene therapy, but it did result in an additional improvement in motor function. These data suggest that a CNS-directed gene therapy approach provides significant clinical benefit, and the addition of the small molecule PPT1 mimetic can further increase that response.

Introduction

Infantile neuronal ceroid lipofuscinosis (INCL) is a rare lysosomal storage disease characterized by progressive neurodegeneration beginning in infancy or childhood (Hofmann et al. 1999; Hofmann and Peltonen 2001; Vesa et al. 1995). INCL is caused by a deficiency in the lysosomal hydrolase palmitoyl protein thioesterase 1 (PPT1). In its absence, cells throughout the CNS and viscera accumulate autofluorescent material, which is

msands@dom.wustl.edu

accompanied by brain atrophy, cortical thinning, widespread neurodegeneration, and glial activation (Das et al. 1998; Hofman et al. 2001; Mitchison et al. 1998, 2004; Vesa et al. 1995). Typically diagnosed by 1.5 years of age, patients with INCL present with clinical features such as blindness, seizures, motor deficits, and cognitive decline. INCL is invariably fatal, and currently there is no treatment available for this disorder (Haltia et al. 1973a, b, 1995; Hofmann and Peltonen 2001; Vanhanen et al. 1997).

Gupta and colleagues (2001) generated a mouse model of INCL, the *Ppt1*-/- mouse. Characterization studies suggest that the mouse model of INCL recapitulates the human course of disease (Bible et al. 2004; Griffey et al. 2004, 2005, 2006; Gupta et al. 2001). At the end stage of life, the *Ppt1*-/- mice suffer from the same pathological changes and functional deficits as patients with INCL. Based on these similarities, the *Ppt1*-/- mouse is an excellent tool for investigating potential therapies for the treatment of INCL.

Lysosomotropic drugs have been suggested as potential therapeutics for treating INCL (Zhang et al. 2001). Since the CNS is the most severely affected organ in INCL and it is a difficult organ to target, a small molecule drug that is bio- available, able to cross the blood brain barrier, enter the lysosome, and disrupt thioester linkages similar to PPT1 would be an ideal candidate for treatment of INCL. Previous in vitro work suggests that the small molecule drug phosphocysteamine might fit these criteria and be a viable option for treating INCL (Zhang et al. 2001). Although in vitro studies suggest that the PPT1 mimetic phosphocysteamine is not as effective at cleaving thioester linkages as endogenous PPT1 (Lu and Hofmann 2006), phosphocysteamine did clear storage material from INCL fibroblasts and prevent substrate reaccumulation (Zhang et al. 2001).

To date, preclinical treatment strategies for INCL have demonstrated partial improvements in disease parameters. Intracranial delivery of gene-based (i.e., adeno-associated virus type 2; AAV2), small molecule–based (i.e., resveratrol), or stem cell-based (i.e., human central nervous system stem cells; hCNSSCs) therapies provide some biochemical, histochemical, and functional improvements (Griffey et al. 2005, 2006; Tamaki et al. 2009; Wei et al. 2011). However, the behavioral improvements were minimal, and no significant increase in survival was reported.

Given the limited efficacy of single treatment regimens in preclinical experiments, we hypothesized that therapies used in combination would better target the complexity of disease in INCL. Since INCL has significant systemic disease (Galvin et al. 2008), and intracranial delivery of gene or stem cell therapies fails to deliver enzyme to the CNS in its entirety, we hypothesized that teaming daily systemic injections of phosphocysteamine with the intracranial delivery of gene therapy at birth would confer a greater therapeutic benefit. Previous work demonstrated that the intracranial delivery of six injections of AAV2-PPT1 at birth in the *Ppt1*-/- mice provided the greatest therapeutic promise (Griffey et al. 2006). Thus, we employed a similar approach in the current study but used adeno-associated virus type 5 (i.e., AAV2/5-PPT1) due to its greater transduction efficiency and distribution levels in the central nervous system (Davidson et al. 2000; Burger et al. 2004). We hypothesized that daily injections of phosphocysteamine would provide the PPT1 mimetic to regions of the CNS that had sub therapeutic levels of PPT1 activity from the CNS- directed gene

therapy alone. Therefore, the combination of the PPT1 mimetic and low levels of *Ppt1* activity might synergize to provide more regions in the CNS with therapeutic compounds that are able to degrade accumulated substrates present in INCL. In addition, the systemic administration of phosphocysteamine would also target the viscera and help reduce the systemic disease to further increase efficacy.

Intracranial injections of AAV2/5 alone result in a significant improvement in histological parameters such as brain weight, autofluorescent accumulation, cortical thickness, and neuroinflammation (Kielar et al. 2007; Macauley et al. 2009). Additional improvements, albeit modest and transient, were seen when phosphocysteamine was combined with AAV2/5. These data provide evidence for long-term clinical, biochemical, and histological improvements in the murine model of INCL and form the basis for effective treatment of this inherited neurodegenerative disease.

Materials and methods

Ppt1-/- and wildtype mice

Ppt1-/- mice were created as previously described on a mixed background (Gupta et al. 2001). Subsequently, the mice were bred to C57Bl/6 mice for 10 generations to produce a congenic strain (Griffey et al. 2004). Wildtype (WT) or *Ppt1*-deficient (*Ppt1*-/-) mice were generated by either heterozygous or homozygous matings and genotype was determined by a PCR-based assay. For this study, both male and female *Ppt1*-/- and wildtype mice were used. Animals were housed under a 12:12 h light:dark cycle and provided food and water ad libitum. All procedures were carried out under an approved IACUC protocol from Washington University School of Medicine.

Lifespan

Both treated *Ppt1*-/- mice and untreated controls (*n*010 per group) were used to assess longevity. The end of life was signaled by either death or a predetermined moribund condition. Criteria for sacrifice included a 25% decrease from maximum body weight, prolapsed penis, or unresponsive- ness to tactile stimuli. Kaplan-Meier analysis was used to measure cumulative survival and determine significant differences ($p<0.05$) in lifespan.

Recombinant AAV production

The rAAV2/5-PPT1 vector used in these studies was as previously described (Griffey et al. 2004). Briefly, the vector contained a chicken β-actin promoter, cytomegalovirus enhancer, the first intron from the chicken β-actin gene, rabbit β-globin polyadenylation signal, cDNA for human *PPT1*, and flanking inverted terminal repeats (ITRs) from AAV2. For the packaging of rAAV2/5-PPT1 virus, the 293 cell line was maintained in a 37°C incubator with 5% CO_2 in Dulbecco's modified Eagle's medium (DMEM) supplemented with 5% fetal bovine serum (FBS), 100 units/ml penicillin, and 100 μg/ml streptomycin. At 24 h prior to transfection, cells were plated at a 30–40% confluence in CellSTACS (Corning, Lowell, MA) resulting in 70–80% confluence at the time of transfection. Both 1.8 mg pXYZ5 (AAV5 capsid) helper plasmid and 0.6 mg rAAV-*Ppt1* transfer plasmid were co-transfected into 293 cells using the calcium phosphate precipitation procedure. After 72 h, cells were

harvested and lysed by three freeze/thaw cycles. The cell lysate was treated with 50U/ml of benzonase followed by iodixanol gradient centrifugation. Subsequently, the iodixanol gradient fraction was further purified using a HiTrap Q for column chromatography. AVivaspin 20 100 K concentrator (Sartorius Stedim, Bohemia, NY) was used to concentrate the eluted virus, and vector titer was determined by Dot blot assay.

Intracranial injections

On post-natal day 1, AAV2/5-PPT1 was intracranially injected into six sites in the *Ppt1*-/- brain using a Hamilton syringe and 30-gauge needle. Two microliters of diluted virus (1×1011vg/ml) was bilaterally injected into the anterior cortex (1 mm rostral to bregma, 2 mm medial/lateral of midline, and 2 mm ventral to the surface of the skull), hippocampus/ thalamus (3.5 mm rostral to bregma, 2 mm medial/lateral of midline, and 2 mm ventral to the surface of the skull), and cerebellum (1 mm rostral to lamda, 1 mm medial/lateral of midline, and 2 mm ventral to the surface of the skull).

Phosphocysteamine injections

Ppt1-deficient mice received daily intraperitonial (IP) injections of phosphocysteamine (Sigma-Aldrich, St. Louis, MO) beginning at 28 days of age and continuing for the duration of their life. A phosphocysteamine solution was made daily in Dulbecco's phosphate buffered saline (dPBS), titered to a pH of 7.5, and injected immediately at a dose of 60 mg/kg. Concurrently, *Ppt1*-/- and WT control mice receiving daily injections of dPBS served as controls.

Treatment groups

Mice were assigned to one of five groups based on the treatment received: (1) AAV: *Ppt1*-/- mice receiving intracranial delivery of AAV2/5-*Ppt1* only, (2) phosphocysteamine: *Ppt1*-/- receiving daily phosphocysteamine injections only, (3) AAV+phosphocysteamine: *Ppt1*-/- receiving both intracranial delivery of AAV2/5-PPT1 and daily phosphocysteamine injections, (4) *Ppt1*: *Ppt1*-/- mice receiving daily dPBS injections, and (5) WT: WT mice receiving daily dPBS injections. Each group contained *n*0 14 mice, composed of both males and females, which were allocated to either behavior and longevity studies (*n*010) or a 7 month time point (*n*04).

Biochemicalanalysis

Seven-month-old mice were sacrificed via lethal injection of euthasol, their brains bisected sagitally, and the left hemi- sphere flash frozen in liquid nitrogen. The hemisphere was homogenized in buffer containing 10 mM Tris (pH07.5), 150 mM NaCl, 1 mM dithiothreitol, and 0.2% Triton X-100 and centrifuged at 14,000 rpms for 1 min. Following centrifugation, the supernatant was removed and used for both *PPT1* and β-glucuronidase (β-gluc) enzyme assays as previously described (Griffey et al. 2004; Sands et al. 1993). For *PPT1* assays, the supernatant was incubated with the fluorescent substrate 4-MU-β-6-thiopalmitoylglucoside for 1 h in a 37°C water bath. The reaction was stopped with 500 μl of a 0.1 M sodium carbonate/sodium bicarbonate buffer. For β-gluc assays, 1–10 μl of supernatant was added to 25 μl of 5 mM 4-methylumbelliferyl-β-D-glucuronide (Sigma, St.

Louis, MO) and incubated at 37°C for 1 h. The reactions were stopped by adding 1 ml of 0.1 M Na_2CO_3. Substrate cleavage was measured at 448 nm emission and 365 nm excitation in a Hitachi F-2000 fluorescence spectrophotometer (Hitachi, Pleasanton, CA) using a standard curve ranging from 0.5 to 5 mM of 4-methylumbelliferone (Sigma, St. Louis, MO). The values were normalized to total protein measured using a Coomasie dye-binding assay (Bio-Rad Laboratories, Hercules, CA).

Cortical thickness

The thickness of the primary somatosensory cortex was determined using StereoInvestigator software (Microbrightfield, Williston, VT). Ten perpendicular lines extending from the white matter to the pial surface were measured from three consecutive Nissl-stained sections spanning the S1BF. One-way ANOVAs followed by Bonferroni post-hoc tests were used to determine statistical significance.

Autofluorescence threshold image analysis

In order to determine the extent of endogenous autofluorescence, three consecutive sections spanning the S1BF were mounted onto a chrome-gelatin coated slide and cover slipped with Vectashield (Vector Laboratories). Ten non- overlapping images from each section were captured at 40× magnification using a Leica SP5 confocal microscope and a 488 nm excitation laser. During image capture, all parameters including laser power, gain and offset settings, and calibration were kept constant. Semi-quantitative thresholding analysis was carried out on these confocal images using Image Pro Plus software (Media Cybernetics) to determine the number of pixels per image that contained autofluorescent storage material.

Immunohistochemistry

Inflammation within the CNS was determined by immunohistochemical staining for the astrocytic marker GFAP and the microglial marker CD68. A series of every sixth free-floating section was stained using a previously described protocol (Bible et al. 2004; Griffey et al. 2004. 2006; Kielar et al. 2009). In short, sections were quenched for endogenous peroxidase activity, rinsed, and subsequently blocked using normal serum prior to overnight incubation in primary anti-sera diluted in TBS with normal serum and 0.3% Triton X-100 (polyclonal rabbit anti-GFAP, 1:4000, DAKO; mono- clonal rat anti-CD68, 1:2,000, AbD Serotec). Following another rinse, sections were incubated in secondary antisera diluted in TBS with normal serum and 0.3% Triton X-100 (biotinylated swine anti-rabbit IgG, 1:1,000, DAKO; biotinylated rabbit anti-rat IgG, 1:1,000, Vector Laboratories). Sections were then incubated with an avidin-biotin complex (Vectastain, Vector Laboratories), and the immunoreactivity was visualised using DAB. Sections were mounted onto chrome-gelatin-coated slides, air-dried, cleared in xylene, and cover slipped with DPX. For the double labeling experiments, the sections were blocked in normal serum prior to an overnight incubation with both anti-GFAP and anti-CD68 as outlined above. Goat anti-rabbit Alexa 633 (Invitrogen) and goat anti-rat Alexa 568 (Invitrogen) were used to fluorescently visualize anti-GFAP and anti-CD68, respectively. Sections were counterstained with DAPI, mounted on a slide, and cover slipped with fluoromount G (SouthernBiotech).

Images of GFAP or CD68 immunoreactivity for semi- quantitative threshold analysis were captured at 40× magnification as described above, using a live video camera (JVC, 3CCD, KY-F55B) mounted onto a Zeiss Axioplan micro- scope. Thirty no overlapping images were captured from three sections through the S1BF. Parameters of light intensity, camera setup, and calibration were kept constant. Semi- quantitative thresholding analysis was carried out on these images using Image Pro Plus software (Media Cybernetics) to determine the number of pixels per image that were immunoreactive for GFAP or CD68, respectively. Statistical significance was determined by a one-way ANOVA and Bonferroni post-hoc test.

Rotarod testing

Congenic *Ppt1*-/- mice (*n*011–14 mice per group) and wild- type littermates (*n*010–14 mice per group) were tested on the rotarod beginning at 6 weeks of age, then at 3 months, and every month thereafter. Latency to fall served as the dependent variable, and trials lasted a maximum of 60 s. At each age, mice underwent three test sessions where each session included a pretest trial on a stationary rod, followed by two test trials on the rocking rotarod. For the rocking rotarod paradigm, mice were placed on the rod programmed to alternate rotating forwards and backwards to final speed of 10 rpms. Each rocking test trial lasted 60 s. Statistical significance was determined using one-way ANOVAs at each time point, followed by a Bonferroni post-hoc test.

Results

Biochemicalanalyses

We performed *PPT1* assays to determine the level of enzyme activity in the *Ppt1*-/- brain following intracranial delivery of AAV2/5-PPT1 (Fig. 1a). While the level of *PPT1* activity in the *Ppt1*-/- brain is largely undetectable, the normal mouse brain contains approximately 212 nmol/ mg/h. Following the intracranial delivery of AAV2/5-PPT1, the treated *Ppt1*-/- brain had *PPT1* levels of approximately 400 nmol/mg/h, a two-fold increase over endogenous *PPT1* levels. There was no significant difference in the specific activity between the AAV only or AAV+phosphocysteamine–treated brains. This elevation in *PPT1* activity represented a significant increase when compared to untreated controls ($p<0.0001$). PPT1 activity was not detected in the mutant brains treated with phosphocysteamine only.

In addition to quantifying the *PPT1* levels in treated brains, we investigated whether AAV-mediated gene therapy successfully decreased secondary elevations in lysosomal enzyme activity, a phenomenon typically observed in lysosomal storage diseases (Fig. 1b). To do this, we performed β-glucuronidase (ß-gluc) assays on the brains from both treated mice and untreated controls. There was a six fold increase in β-gluc activity in the brains of *Ppt1*-/- mice compared to WT controls. Following intracranial delivery of AAV2/5-PPT1, there was a significant decrease in β-gluc activity, which was restored to normal levels.

Cortical thickness

Patients suffering from INCL and *Ppt1*-deficient mice display significant cortical atrophy (Bible et al. 2004; Haltia et al. 1973a; Kielar et al. 2007). Therefore, we sought to investigate the effects of treatment on cortical thinning in the treated *Ppt1*-/- mice (Fig. 2).

Upon gross examination, there is pronounced atrophy of the cortical mantle in the *Ppt1*-/- mice compared to WT controls, as is evident in the S1BF cortex (Fig. 2a). When quantified, the thickness of the S1BF cortex from Ppt1-/- mice is decreased by approximately 20% when compared to normal (Fig. 2b). However, there was a significant increase in cortical volume in mice treated with either AAV alone or AAV + phosphocysteamine compared to untreated *Ppt1*-/- mice ($p < 0.0001$). Only an 8–10% decrease in the thickness of the S1BF was present in both the AAV and AAV+phosphocysteamine–treated mice. Compared to wild type brains, there was a significant difference in the AAV only and AAV + phosphocysteamine groups. In contrast, the phosphocysteamine-treated mice showed no improvement in cortical thickness and were indistinguishable from untreated *Ppt*-/- mice.

Brain atrophy

Brain weights were used as a measure of overall brain atrophy (Fig. 2c). By 7 months of age, there was a significant decrease in the brain weights of the *Ppt1*-/- mice compared to WT controls ($p<0.001$) in which the *Ppt1*-/- mice lost approximately24% of their brain mass. However, the brain weights of AAV only and AAV+phosphocysteamine–treated mice at 7 months were 90% of normal, illustrating a significant increase ($p<0.001$) in brain mass compared to untreated *Ppt1*-/- mice. However, at a terminal time point, this therapeutic benefit was lost, and the brain weights of AAV only and AAV+phosphocysteamine–treated brains at approximately 15 months of age were indistinguishable from 7-month-old untreated *Ppt1*-/- mice. Daily treatment with phosphocysteamine alone did not significantly improve brain weights when compared to untreated *Ppt1*-/- mice.

Autofluorescent storage accumulation in the cortex

Accumulation of autofluorescent storage material throughout the neuraxis is a predominant feature of INCL (Fig. 2d). As another measure of therapeutic efficacy, we investigated the levels of autofluorescent storage material in the S1BF cortex in treated mice compared to untreated controls. The AAV only and AAV+phosphocysteamine combination therapy showed a significant reduction ($p<0.05$) in autofluorescent storage material within the S1BF cortex. This storage material was reduced by 96 and 81%, respectively, in the AAV and combination therapy groups.

Neuroinflammatory response in the cortex

A major component of INCL is the neuroinflammatory response characterized by an early astrocyte activation and later stage microglial reactivity (Kielar et al. 2007; Macauley et al. 2009). We therefore performed GFAP and CD68 immunohistochemsitry to investigate whether each therapy had an effect on astrocyte and microglial activation, respectively (Fig. 3). Gross examination of sections stained with GFAP and CD68 (Fig. 3a and b, respectively), revealed a marked increase in immunoreactivity for both markers within the S1BF cortex of *Ppt1*-/- mice when compared to WT controls. Following therapy with AAV alone or AAV+phosphocysteamine, there appeared to be fewer GFAP+or CD68+ cells within the S1BF cortex. To quantify this effect, we used thresholding image analysis to assess the level of GFAP and CD68 immunoreactivity within the S1BF cortex of treated and untreated brains (Fig. 3c and d). Compared to WT controls, there was a significant increase

in immunoreactivity for both GFAP and CD68 within the S1BF of both the untreated *Ppt1*-/- and phosphocysteamine-treated brains. However, there was a significant decrease in GFAP and CD68 immunoreactivity in both AAV only and AAV+phosphocysteamine combination therapy mice ($p<0.0001$), with an increase in GFAP+immunoreactivity in the AAV +phophocysteamine group compared to AAVonly (Fig. 3c). To visualize both the autofluorescent storage accumulation and glial activation in the treated mice, we performed fluorescent double labeling experiments with anti-GFAP and anti-CD68, markers of reactive astrocytes and activated microglia, respectively, in the S1BF cortex (Fig. 4). Al- though no autofluorescent storage material and glial activation were present in WT mice, the S1BF cortex of *Ppt1-/-* mice displayed a significant increase in storage material, astrogliosis, and microglial activation. The insets demonstrate that although storage material was found in microglia, the majority of storage products seem to localize to other cell types, presumably neurons. There is still auto- fluorescent accumulation present in phosphocysteamine- treated mice in addition to high levels of anti-GFAP and anti-CD68 immunoreactivity. Treatment with either AAVor AAV+phosphocysteamine results in a dramatic decrease in autofluorescent accumulation, astrogliosis, and microglial activation.

Motor function

To determine whether AAV2/5-mediated gene therapy in combination with phosphocysteamine corrected functional deficits associated with INCL, we tested the mice monthly on a rocking rotorod paradigm (Fig. 5a). At 5 months of age, all groups performed comparably on this paradigm. By 6 months of age, the performance of phosphocysteamine-treated mice and untreated *Ppt1*-/- controls began to diminish. However, the performance of phosphocysteamine-treated mice was significantly better than that of the untreated *Ppt1*-/- mice at this time point ($p<0.001$). The performances of both the AAVonly and AAV +phosphocysteamine–treated groups were indistinguishable from WT at this time point. By 7 months of age, the phosphocysteamine-treated group performed as poorly as the *Ppt1*-/- mice with both groups unable to stay on the rod for more than 10 s. In contrast, between 5 and 7 months of age, the performance of both the AAV only and AAV+phosphocysteamine group steadily improved. Notably, the motor function of the AAV+ phosphocysteamine group was indistinguishable from WT at 7 months of age, as well as being significantly improved compared to AAV only–treated mice. This discrepancy in performance between the AAVand AAV+phosphocysteamine group continued through the 8-month time point, demonstrating an interim benefit of the additional phosphocysteamine treatment. This benefit is most likely due to a decreased variability in performance (Fig. 5b). The scatter plot at 7 months demonstrates the variability in performance in the AAV only treatment group compared to the AAV+phophocysteamine group. By 9 months of age, the latency to fall for both groups continued to plummet until they reached a nadir in performance at 11 months of age. Between 9 and 12 months of age, no significant difference in the performance of AAV only and AAV+phosphocysteamine groups was appreciable. In comparison, the WT mice performed at criterion (60 s) for the duration of the testing period.

Lifespan

We also investigated the effects of different treatment strategies on lifespan in the *Ppt1*-/- mouse (Fig. 6). Similar to previous findings (Griffey et al. 2004; Gupta et al. 2001) the

Ppt1-/- mice died prematurely (median survival 0 36.5 weeks) when compared to normal littermates. Treatment with either AAV only or AAV+phosphocysteamine significantly increased the survival of the *Ppt1*-/- mice when compared to untreated littermates ($p<0.0001$). The median survival for the AAV+ phosphocysteamine group was 59 weeks compared to 54 weeks in the AAV only– treated group; however, this difference in longevity was not statistically significant. The median survival for the phosphocysteamine-treated mice was 34 weeks of age, thus demonstrating no improvement in lifespan when compared to the untreated *Ppt1*-/-mice.

Discussion

In this study, we evaluated the efficacy of combination treatment for INCL using CNS-directed AAV-mediated gene therapy teamed with the lysosomotropic drug phosphocysteamine. Previous experiments that directed treatment of AAV2-mediated gene therapy to the brain provided some promise in a mouse model of INCL. There were measurable improvements on many biochemical and histological parameters, but the functional improvement was modest, and no significant increase in lifespan was observed. In this experiment, we substituted AAV2/5 for AAV2 due to its greater transduction efficiency and higher expression level in the CNS, potentially making it a better choice for treating INCL. In fact, treatment with AAV2/5- PPT1 alone resulted in the greatest histological, biochemical, and functional improvements of any single therapy to date in INCL. Following AAV-mediated gene therapy, the *Ppt1*-/- mice had increased brain mass, decreased cortical thinning, decreased autofluorescent accumulation, and decreased neuroinflammation in the CNS. Furthermore, there were sustained improvements on the rocking rotarod test beginning at 6 months. Previous studies using small- molecule drugs, gene therapy, or neuronal stem cells resulted in significant improvements in motor function, but this was only maintained for a short duration (Griffey et al. 2006; Tamaki et al. 2009; Wei et al. 2011). Finally, there was a substantial improvement in lifespan in the AAVonly–treated mice to 54 from 36 weeks. Previously, the only documented increase in lifespan in this model was described with the use of resveratrol and that consisted of a 2-week increase in longevity (Wei et al. 2011).

Although AAV2/5-mediated gene therapy provided the best singular therapeutic benefit reported to date, its efficacy was still only partial. Therefore, we hypothesized that using AAV2/5 in combination with other therapies would maximize the treatment outcomes in INCL. One of the limitations of intraparencymal injections of viral vectors is that the area of correction is largely localized to the injection site (Passini et al. 2005). Since the CNS disease in INCL is widespread (Bible et al. 2004), finding a therapy that increases the area of correction would have enormous potential. Furthermore, previous reports describe significant storage pathology within the visceral organs in addition to the CNS (Galvin et al. 2008; Haltia et al. 1973a; Hofman et al. 2001). Therefore, addition of a complementary therapy that also has the potential to treat the systemic disease might be expected to increase efficacy. Thus, we investigated the use of the small lysosomotropic drug and PPT1 mimetic phosphocysteamine as an adjunct therapy for INCL to be used in combination with gene therapy.

Since phosphocysteamine can disrupt thioester linkages on palmitoylated proteins in human INCL fibroblasts (Lu and Hofmann 2006; Zhang et al. 2001), it seemed to be an ideal candidate for an adjunct therapy for INCL. In order for a small molecule such as phosphocysteamine to be successful, it needs to be bioavailable, cross the blood-brain barrier, and traffic to the lysosome; all characteristics that have been attributed to phosphocysteamine (Zhang et al. 2001). How- ever, the therapeutic improvement in the *Ppt1*-/-mouse from daily dosing with phosphocysteamine was both minimal and transient. Phosphocysteamine-alone provided an incremental but significant improvement on rotarod function at 6 months of age, although brain atrophy, cortical thinning, and glial activation remained unchanged. There was a slight decrease in autofluorescent accumulation with phosphocysteamine alone but it did not reach statistical significance. Nonetheless, the apparent decrease in storage material is consistent with the small but significant improvement in motor function.

The most notable improvement reported with the combination of AAV+phosphocysteamine therapy in comparison to AAValone was also seen in the rocking rotarod paradigm. Although the histological improvements seen in both the AAV and AAV +phosphocysteamine groups were impressive, they were not significantly different from one another, suggesting that the majority of improvement was due to AAV2/5 and not the combination approach. However, at both 7 and 8 months of age, the motor performance of the AAV+phosphocysteamine group was significantly better than the AAVonly group. This is an important finding since functional improvements are perhaps the most meaningful measure of clinical efficacy.

Similarly, there was a trend towards an increased lifespan (~5 weeks) in the combination treatment group compared to the AAV only group. These data suggest that although the addition of phosphocysteamine to the AAV treatment regimen did not provide any further improvement in biochemical and histological measures, phosphocysteamine did have a meaningful, albeit transient, clinical effect if given together with gene therapy. Finally, although phosphocysteamine provided only an incremental increase in efficacy, a more complete response might be achieved if using a higher dose, a different method of drug delivery, or a different treatment regimen.

In this study, we proposed a combination therapy approach for the treatment of INCL. This study demonstrated that treatment with either AAVonly or AAV+phosphocysteamine can improve histological parameters, behavioral function, and longevity in the *Ppt1*-/- mice. Furthermore, we would argue that the combination therapy of AAV and phosphocysteamine was more beneficial than either therapy alone based on the interim functional improvement on the rotarod. These preclinical findings provide a basis for future clinical trials for INCL.

Acknowledgments

We would like to thank Beth Eultgen for her help with animal husbandry. This study was supported by NIH grants (NS043105; MSS), Ruth L. Kirschstein NRSA Fellowship (NS056728; SLM), The Wellcome Trust (GR079491MA; JDC, AMW, DY), Batten Disease Family Association (JDC, AMW, DY), the Batten Disease Support and Research Association (JDC, AMW, DY, SLM, MSS), and the Bletsoe Family (JDC, AMW).

References

Bible E, Gupta P, Hofmann SL, Cooper JD. Regional and cellular neuropathology in the palmitoyl protein thioesterase-1 null mutant mouse model of infantile neuronal ceroid lipofuscinosis. Neurobiol Dis. 2004; 16:346–359. [PubMed: 15193291]

Burger C, Gorbatyuk OS, Velardo MJ, Peden CS, Williams P, Zolotukhin S, Reier PJ, Mandel RJ, Muzyczka N. Recombinant AAV viral vectors pseudo typed with viral capsids from serotypes 1, 2, and 5 display differential efficiency and cell tropism after delivery to different regions of the central nervous system. Mol Ther. 2004; 10:302–317. [PubMed: 15294177]

Das AK, Becerra CH, Yi W, Lu JY, Siakotos AN, Wisniewski KE, Hofmann SL. Molecular genetics of palmitoyl-protein thioesterase deficiency in the U.S. J Clin Invest. 1998; 102:361–370. [PubMed: 9664077]

Davidson BL, Stein CS, Heth JA, Martins I, Kotin RM, Derksen, Zabner J, Ghodsi A, Chiorini JA. Recombinant adeno-associated virus type 2, 4, and 5 vectors: transduction of variant cell types and regions in the mammalian central nervous system. Proc Natl Acad Sci. 2000; 97:3428–3432. [PubMed: 10688913]

Galvin N, Vogler C, Levy B, Kovacs A, Griffey M, Sands MS. A murine model of infantile neuronal ceroid lipofuscinosis ultra structural evaluation of storage in the central nervous system and viscera. Pediatr Dev Pathol. 2008; 11:185–192. [PubMed: 17990914]

Griffey M, Bible E, Vogler C, Levy B, Gupta P, Cooper J, Sands MS. Adeno-associated virus 2-mediated gene therapy decreases autofluorescent storage material and increases brain mass in a murine model of infantile neuronal ceroid lipofuscinosis. Neurobiol Dis. 2004; 16:360–369. [PubMed: 15193292]

Griffey M, Macauley SL, Ogilvie JM, Sands MS. AAV2-mediated ocular gene therapy for infantile neuronal ceroid lipofuscinosis. Mol Ther. 2005; 12:413–421. [PubMed: 15979943]

Griffey MA, Wozniak D, Wong M, Bible E, Johnson K, Rothman SM, Wentz AE, et al. CNS-directed AAV2-mediated gene therapy ameliorates functional deficits in a murine model of infantile neuronal ceroid lipofuscinosis. Mol Ther. 2006; 13:538–547. [PubMed: 16364693]

Gupta P, Soyombo AA, Atashband A, Wisniewski KE, Shelton JM, Richardson JA, Hammer RE, et al. Disruption of PPT1 or PPT2 causes neuronal ceroid lipofuscinosis in knockout mice. Proc Natl Acad Sci USA. 2001; 98:13566–13571. [PubMed: 11717424]

Haltia M, Rapola J, Santavuori P. Infantile type of so-called neuronal ceroid-lipofuscinosis. Histological and electron microscopic studies. Acta Neuropathol (Berl). 1973a; 26:157–170. [PubMed: 4763201]

Haltia M, Rapola J, Santavuori P, Keranen A. Infantile type of so-called neuronal ceroid lipofuscinosis. 2. Morphological and biochemical studies. J Neurol Sci. 1973b; 18:269–285. [PubMed: 4121459]

Haltia M, Tyynela J, Baumann M, Henseler M, Sandhoff K. Immunological studies on sphingolipid activator proteins in the neuronal ceroid-lipofuscinoses. Gerontology. 1995; 41(Suppl 2):239–248. [PubMed: 8821335]

Hofmann, SL.; Peltonen, L. The neuronal ceroid lipofuscinosis.. In: Scriver, CR.; Beaudet, AL.; Sly, WS.; Valle, D., editors. The metabolic and molecular basis of inherited disease. McGraw-Hill; New York: 2001. p. 3877-3894.

Hofmann SL, Das AK, Yi W, Lu JY, Wisniewski KE. Genotype-phenotype correlations in neuronal ceroid lipofuscinosis due to palmitoyl-protein thioesterase deficiency. Mol Genet Metab. 1999; 66:234–239. [PubMed: 10191107]

Hofman IL, van der Wal AC, Dingemans KP, Becker AE. Cardiac pathology in neuronal ceroid lipofuscinosis—a clinico-pathologic correlation in three patients. Eur J Paediatr Neurol. 2001; 5(Suppl A):213–217. [PubMed: 11589001]

Kielar C, Maddox L, Bible E, Pontikis CC, Macauley SL, Griffey MA, Wong M, et al. Successive neuron loss in the thalamus and cortex in a mouse model of infantile neuronal ceroid lipofuscinosis. Neurobiol Dis. 2007; 25:150–162. [PubMed: 17046272]

Kielar C, Wishart TM, Palmer A, Dihanich S, Wong AM, Macauley SL, Chan CH, et al. Molecular correlates of axonal and synaptic pathology in mouse models of Batten disease. Hum Mol Genet. 2009; 18:4066–4080. [PubMed: 19640925]

Lu JY, Hofmann SL. Inefficient cleavage of palmitoyl-protein thioesterase (PPT) substrates by aminothiols: implications for treatment of infantile neuronal ceroid lipofuscinosis. J Inherit Metab Dis. 2006; 29:119–126. [PubMed: 16601878]

Macauley SL, Wozniak DF, Kielar C, Tan Y, Cooper JD, Sands MS. Cerebellar pathology and motor deficits in the palmitoyl protein thioesterase1-deficient mouse. Exp Neurol. 2009; 217:124–135. [PubMed: 19416667]

Mitchison HM, Hofmann SL, Becerra CH, Munroe PB, Lake BD, Crow YJ, Stephenson JB, et al. Mutations in the palmitoyl-protein thioesterase gene (PPT; CLN1) causing juvenile neuronal ceroid lipofuscinosis with granular osmiophilic deposits. Hum Mol Genet. 1998; 7:291–297. [PubMed: 9425237]

Mitchison HM, Lim MJ, Cooper JD. Selectivity and types of cell death in the neuronal ceroid lipofuscinoses. Brain Pathol. 2004; 14:86–96. [PubMed: 14997941]

Passini MA, Macauley SL, Huff MR, Taksir TV, Bu J, Wu IH, Piepenhagen PA, et al. AAV vector-mediated correction of brain pathology in a mouse model of Niemann-Pick A disease. Mol Ther. 2005; 11:754–762. [PubMed: 15851014]

Sands MS, Barker J, Vogler C, Levy B, Gwynn B, Galvin N, Birkenmeier EH. Treatment of murine mucopolysaccharidosis type VII in newborns by syngeneic bone marrow transplantation. Lab. Invest. 1993; 68:676–686. [PubMed: 8515654]

Tamaki SJ, Jacobs Y, Dohse M, Capela A, Cooper JD, Reitsma M, He D, et al. Neuroprotection of host cells by human central nervous system stem cells in a mouse model of infantile neuronal ceroid lipofuscinosis. Cell Stem Cell. 2009; 5:310–319. [PubMed: 19733542]

Vanhanen SL, Sainio K, Lappi M, Santavuori P. EEG and evoked potentials in infantile neuronal ceroid lipofuscinosis. Dev Med Child Neurol. 1997; 39:456–463. [PubMed: 9285436]

Vesa J, Hellsten E, Verkruyse LA, Camp LA, Rapola J, Santavuori P, Hofmann SL, et al. Mutations in the palmitoyl protein thioesterase gene causing infantile neuronal ceroid lipofuscinosis. Nature. 1995; 376:584–587. [PubMed: 7637805]

Wei H, Zhang Z, Saha A, Peng S, Chandra G, Quezado Z, Mukherjee AB. Disruption of adaptive energy metabolism and elevated ribosomal p-S6K1 levels contribute to INCL pathogenesis: partial rescue by resveratrol. Hum Mol Genet. 2011; 20:1111–1121. [PubMed: 21224254]

Zhang Z, Butler JD, Levin SW, Wisniewski KE, Brooks SS, Mukherjee AB. Lysosomal ceroid depletion by drugs: therapeutic implications for a hereditary neurodegenerative disease of childhood. Nat Med. 2001; 7:478–484. [PubMed: 11283676]

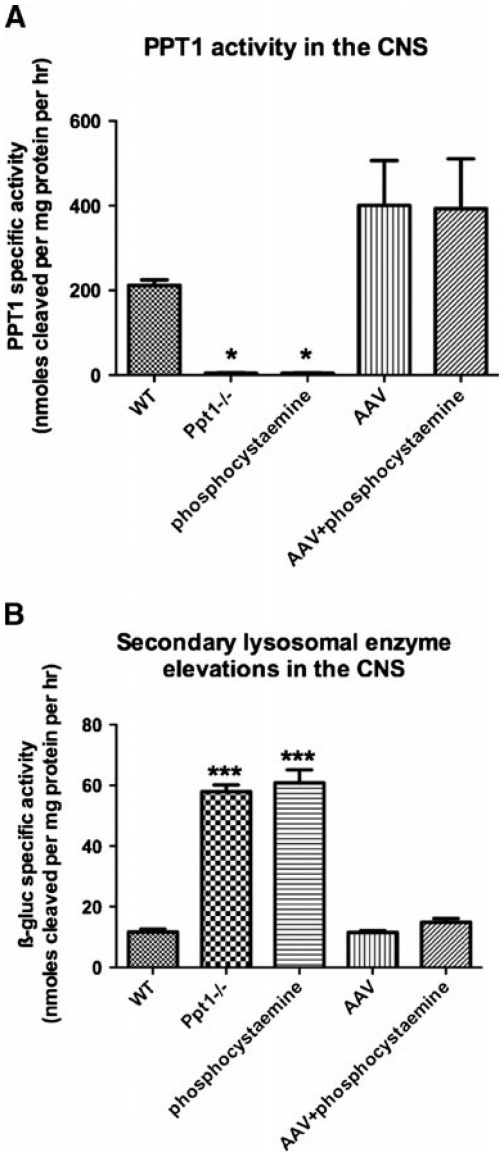

Fig. 1a, b.

PPT1 activity and secondary lysosomal enzyme elevations in the brain at 7 months of age. a PPT1 activity in the treated and untreated brains. *Ppt1*-/- mice treated with either AAV only or AAV+ phosphocysteamine resulted in a twofold increase in PPT1 enzyme activity compared to WT brains. Untreated *Ppt1*-/- brains or those treated with only phosphocysteamine had undetectable levels of PPT1 activity in the brain. b Secondary lysosomal enzyme elevations in the treated and untreated brains. To ascertain whether secondary elevations in lysosomal enzyme activity were decreased in response to therapy, we performed β-glucoronidase activities on the brains from treated and untreated mice. There was a six fold increase in β-glucoronidase activity in the brains of untreated *Ppt1*-/- mice compared to normal. A similar increase in β-glucoronidase activity was observed in the phosphocysteamine only group. Following either AAV only or AAV+phosphocysteamine

treatment, there was a decrease in secondary enzyme elevation, returning β-glucoronidase activity to WT levels. (*p<0.05, ***p<0.001)

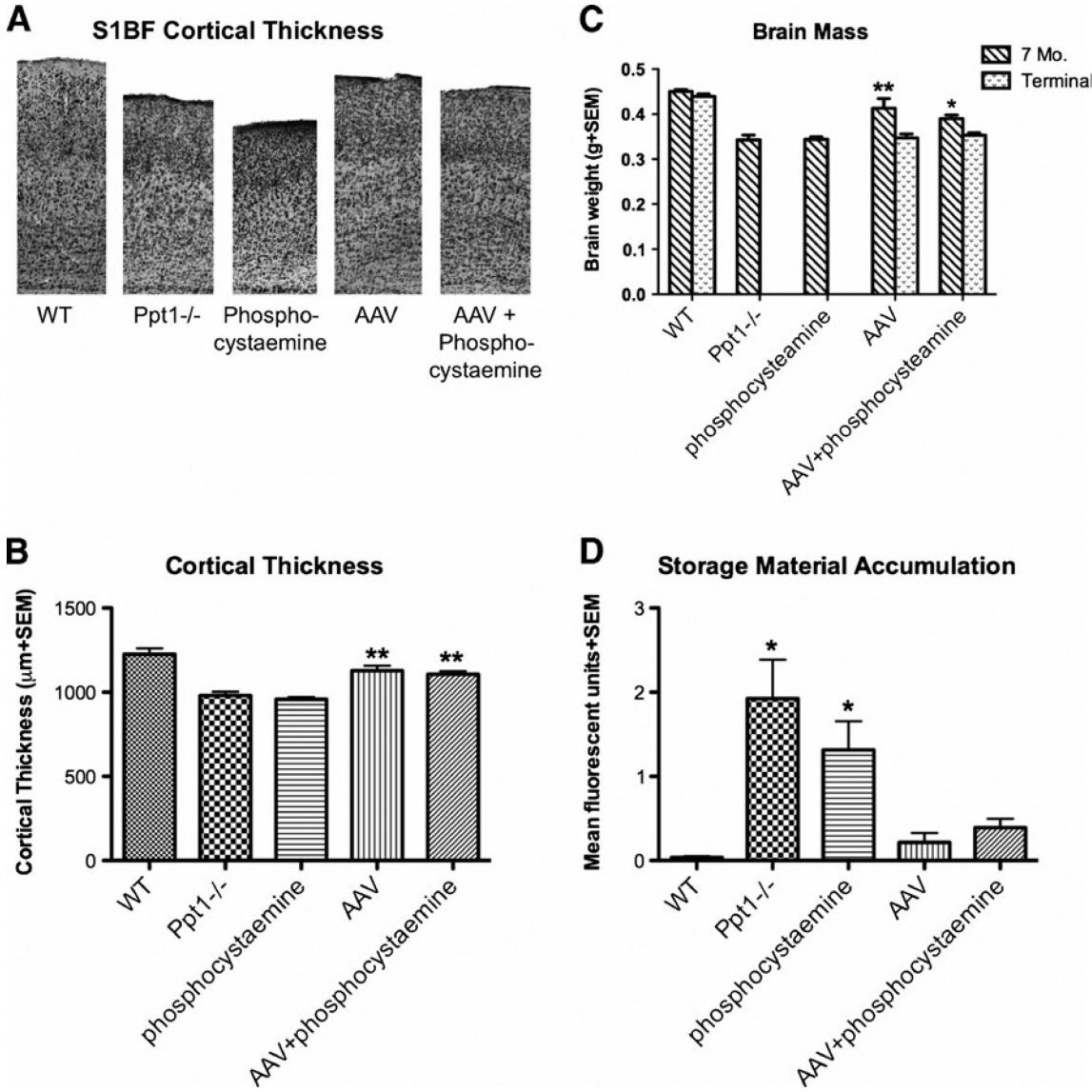

Fig. 2a-d.

Histological improvement in the cortex following therapy. a Representative micrographs of the S1BF cortex at 7 months. Nissl- stained sections reveal the pronounced thinning of the primary somato- sensory cortex (S1BF) of *Ppt1*-/- mice compared to WT controls. Mutant mice treated with phosphocysteamine display a similar level of cortical thinning as the *Ppt1*-/- mice. Treatment with either AAV only or AAV+phophocysteamine appeared to prevent the thinning of S1BF. b Cortical thickness measurements at 7 months. Both the *Ppt1*-/- group and the phosphocysteamine-treated mutant mice displayed a significant thinning of the S1BF compared to WT mice. Following treatment, the AAV only and AAV +phosphocysteamine treatment groups both exhibited a significant increase in cortical thickness when compared to untreated *Ppt1*-/- mice. c Overall brain atrophy in the treated and untreated mice at 7 months and terminal time points. *Ppt1*-/- mice display a significant reduction in brain mass at 7 months of age in comparison to WT mice. A similar reduction in brain mass was seen in phosphocysteamine-treated mutant mice. Notably, the AAVonly

and AAV+phosphocysteamine–treated mutant mice displayed a significant increase in brain mass at 7 months of age. However, this therapeutic benefit was lost at a terminal time point in both treated groups. d Auto- fluorescent storage material accumulation in 7 month S1BF cortex of treated and untreated mice. Compared to WT mice, untreated *Ppt1*-/- mice and phosphocysteamine only groups display a significant accumulation of autofluorescent storage material within the S1BF cortex. Following treatment, there is a significant reduction in autofluorescent material in the AAV only and AAV+phosphocysteamine groups. (*p< 0.05, **p<0.01, n.s. 0 no significant difference)

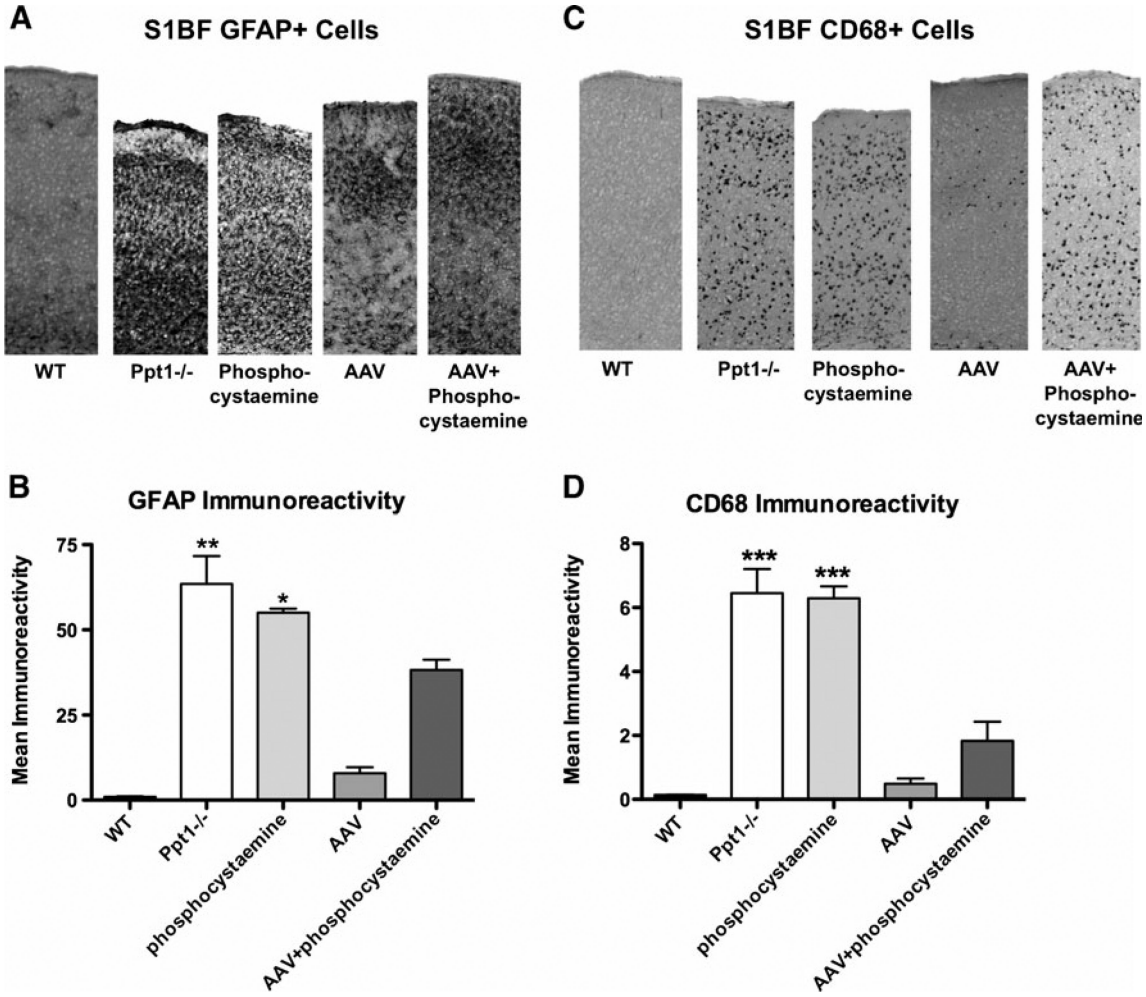

Fig. 3a-d.

Decreased neuroinflammation following therapeutic intervention. a Astrocyte activation in the S1BF cortex at 7 months. Untreated *Ppt1*-/-mice and phosphocysteamine-treated mice display pronounced GFAP staining in the S1BF cortex, indicative of astrocyte activation in this brain region. This was reduced following AAV only or AAV+phosphocysteamine treatment. b Quantification of GFAP immunoreactivity in the S1BF cortex at 7 months. Thresholding image analysis reveals a significant increase in GFAP immunoreacitvity in the S1BF of both untreated *Ppt1*-/- and phosphocysteamine-treated mice compared to WT controls. Treatment with either AAV only or AAV+ phosphocysteamine resulted in a significant decrease in GFAP immunoreactivity within the S1BF. Notably, AAV +phosphocysteamine–treated mice still displayed significant elevations in GFAP staining compared to AAV only–treated mutant mice. c Microglial activation in the S1BF cortex at 7 months. Staining for CD68 revealed a pronounced increase in staining in the S1BF cortex of *Ppt1*-/- mice compared to WTcontrols. A similar pattern of CD68 immunoreactivity was apparent in the phosphocysteamine-treated mice. Conversely, the S1BF of *Ppt1*-/- mice treated with either AAVonly or AAV+phosphocysteamine appeared to have fewer, less intensely stained CD68+ cells than were seen in untreated mutants. d Quantification of CD68 immunoreactivity in the S1BF cortex at 7 months. Both the *Ppt1*-/- and

phosphocysteamine-treated mice displayed significantly more CD68 staining in the S1BF compared to WT controls. Relative to untreated *Ppt1*-/- mice, treatment with either AAV only or AAV+phosphocysteamine resulted in a significant reduction in the level of CD68 immunoreactivity in the S1BF. (*p<0.05, **p<0.01, ***p<0.001)

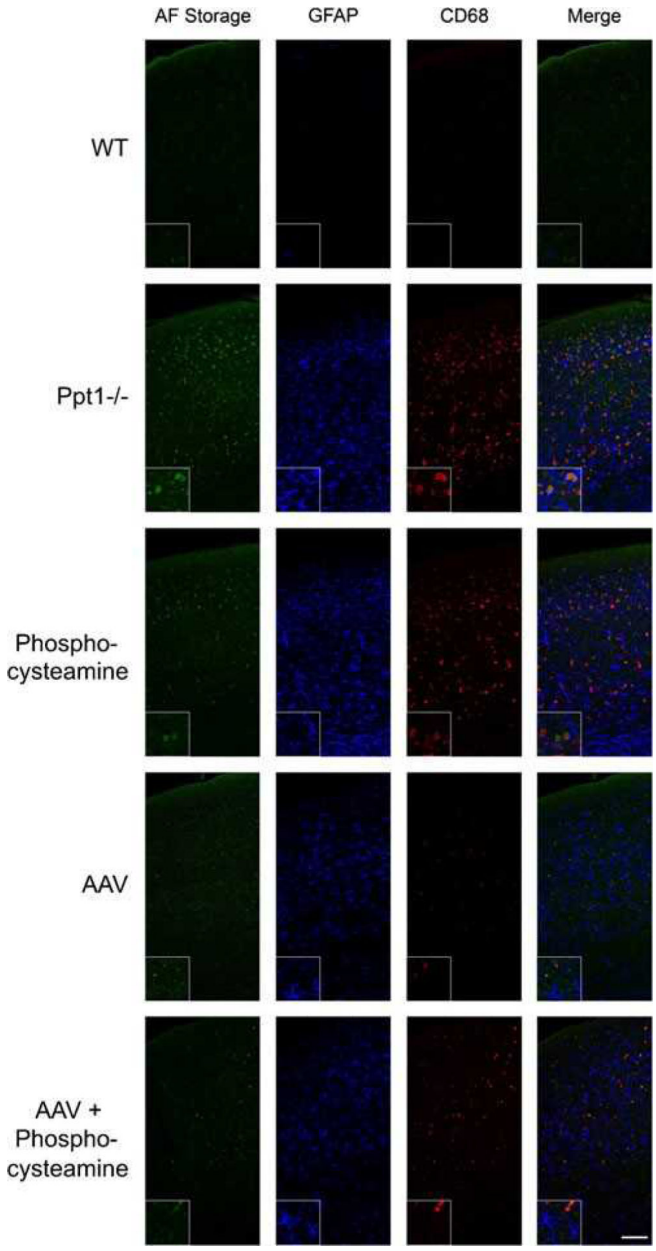

Fig. 4.

Autofluorescent storage material accumulation, astrocytosis, and microglia activation in treated and untreated *Ppt1-/-* mice. Fluorescent micrographs of autofluorescent storage, GFAP+astrocytes, and CD68+ microglia in the S1BF cortex of WT, *Ppt1-/-* , phosphocysteamine-treated, AAV-treated, and AAV+phosphocysteamine–treated *Ppt1-/-* mice. No autofluorescent accumulation or glial activation is present in the WT mice at 7 months of age. Conversely, there are high levels of autofluorescent accumulation in the S1BF cortex of untreated *Ppt1-/-* mice, which coincides with both astrocyte (GFAP) and microglial (CD68) upregulation. In the *inset*, note that there is more autofluorescent accumulation within CD68+ cells than GFAP+cells, although the majority of storage material appears to be localized to another cell type, most likely the neurons. The storage

material in phosphocysteamine-treated mice appears less than the untreated *Ppt1-/-* mice, while treatment with phosphocysteamine does not appear to affect GFAP or CD68 levels in the S1BF. Conversely, treatment with either AAVonly or AAV+phosphocysteamine resulted in decreased autofluorescence, GFAP+immunostaining, and CD68+ immunostaining. *Scale bar* 0100 μm

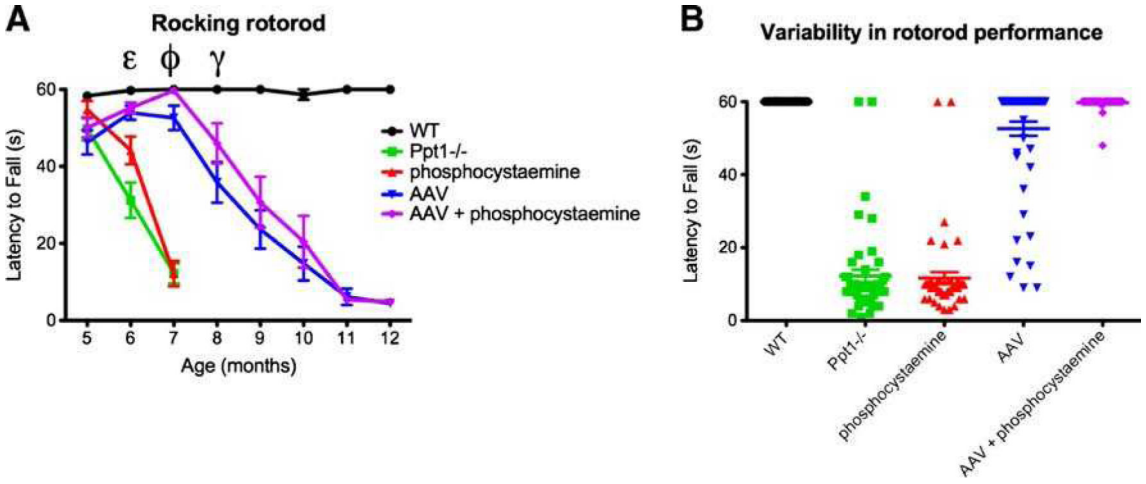

Fig. 5a, b.

Functional improvement on the rocking rotorod paradigm. a Motor improvement observed following therapeutic intervention. At 5 months of age, all treated and untreated mice performed similarly on the rocking rotorod paradigm. At 6 months, the performance of the phosphocysteamine only and untreated *Ppt1*-/- mice began to deteriorate and was significantly worse compared to WTcontrols ($p<0.0001$). Phosphocysteamine-treated mutant mice performed better at 6 months of age compared to untreated *Ppt1*-/- mice (ε). Remarkably, the performance of the AAV only or AAV+phosphocysteamine treated–mice was comparable to W T. The motor function of both phosphocysteamine-treated and untreated *Ppt1*-/- mice deteriorated dramatically by 7 months of age. At 7 months, AAV +phosphocysteamine–treated mice not only performed significantly better than AAV only–treated mice ($p<0.001$), but the motor performance of the combination group was indistinguishable from WT (φ). At 8 months, motor function in AAV only and AAV +phosphocysteamine–treated mice began to decline, but the performance of the AAV +phophocysteamine treatment group was still significantly improved compared to AAV only–treated mutant mice (γ; $p<0.05$). Motor performance continued to decline in both the AAVonly and AAV+ phophocysteamine–treated mice until they were unable to accomplish this task at 12 months of age. b Scatter plot of rocking rotorod data for 7-month-old mice. Each *point* represents an individual trial for each mouse tested within each treatment group. In the WT group, all mice stayed on the rod for 60 s. In comparison, the phosphocysteamine and untreated *Ppt1*-/- mice performed poorly, and each individual trial clustered around 10 s. Of particular interest is the comparison between the AAV only and AAV +phosphocysteamine groups. The variability within the AAV only treatment group was far greater than the AAV+phosphocysteamine group, suggesting that combination therapy was more effective than AAV treatment alone

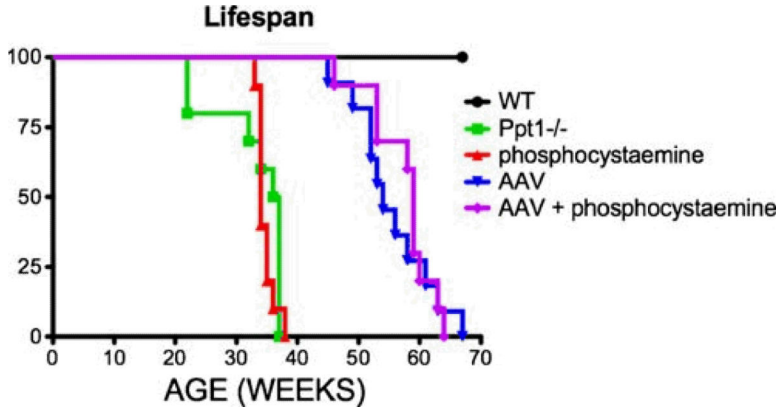

Fig. 6.

Improvement in lifespan following AAV-mediated gene therapy with or without phosphocysteamine. The median lifespan of the untreated *Ppt1*-/-mice was 36.5 weeks compared to 34 weeks in the phosphocysteamine-treated mutant mice. There was a significant improvement in lifespan in mutant mice treated with either AAV only or AAV +phosphocysteamine. Treatment with AAV only increased their median lifespan to 54 weeks while AAV+ phosphocysteamine increased median lifespan to 59 weeks, although this difference was not significant